Smart Structures and Systems, Vol. 8, No. 1 (2011) 119-137

DOI: http://dx.doi.org/10.12989/sss.2011.8.1.119

Implementation of a bio-inspired two-mode structural health monitoring system

Tzu-Kang Lin*[1], Li-Chen Yu[2], Chang-Hung Ku[2], Kuo-Chun Chang[2] and Anne Kiremidjian[3]

[1]National Center for Research on Earthquake Engineering, Taiwan
[2]Department of Civil Engineering, National Taiwan University, Taiwan
[3]Department of Civil and Environmental Engineering, Stanford University, USA

(Received April 18, 2010, Accepted October 20, 2010)

Abstract. A bio-inspired two-mode structural health monitoring (*SHM*) system based on the Naïve Bayes (*NB*) classification method is discussed in this paper. To implement the molecular biology based Deoxyribonucleic acid (*DNA*) array concept in structural health monitoring, which has been demonstrated to be superior in disease detection, two types of array expression data have been proposed for the development of the *SHM* algorithm. For the micro-vibration mode, a two-tier auto-regression with exogenous (*AR-ARX*) process is used to extract the expression array from the recorded structural time history while an *ARX* process is applied for the analysis of the earthquake mode. The health condition of the structure is then determined using the *NB* classification method. In addition, the union concept in probability is used to improve the accuracy of the system. To verify the performance and reliability of the *SHM* algorithm, a downscaled eight-storey steel building located at the shaking table of the National Center for Research on Earthquake Engineering (*NCREE*) was used as the benchmark structure. The structural response from different damage levels and locations was collected and incorporated in the database to aid the structural health monitoring process. Preliminary verification has demonstrated that the structure health condition can be precisely detected by the proposed algorithm. To implement the developed *SHM* system in a practical application, a *SHM* prototype consisting of the input sensing module, the transmission module, and the *SHM* platform was developed. The vibration data were first measured by the deployed sensor, and subsequently the *SHM* mode corresponding to the desired excitation is chosen automatically to quickly evaluate the health condition of the structure. Test results from the ambient vibration and shaking table test showed that the condition and location of the benchmark structure damage can be successfully detected by the proposed *SHM* prototype system, and the information is instantaneously transmitted to a remote server to facilitate real-time monitoring. Implementing the bio-inspired two-mode *SHM* practically has been successfully demonstrated.

Keywords: structural health monitoring; naive bayes; bio-inspired; prototype system.

1. Introduction

Recently, an increasing number of infrastructures and buildings all over the world have been unexpectedly damaged or have collapsed due to aging and long-term material degradation. Even though most of these structures have been periodically examined or monitored using modern

*Corresponding Author, Research Fellow, E-mail: tklin@ncree.org

techniques, these catastrophic failures continue to happen. Due to the existence of a large number of aging buildings, structural health monitoring (*SHM*) has become an important issue in civil engineering and must go hand in hand with the current research to improve the capacity of structures and to develop a safer design method.

The multidisciplinary research field of *SHM* was first proposed in the area of aerospace engineering. Accompanied by the development of advanced sensors, *SHM* was then subsequently developed for applications such as aerospace engineering, mechanical engineering, and civil engineering. However, contrary to the other two fields, civil engineering has faced specific challenges with respect to *SHM* development. For example, large-scale monitoring applications in civil engineering, often using customized monitoring equipment, make monitoring a difficult task. Unlike the mass production frequently seen in the field of mechanical engineering where a specific *SHM* module can be applied to all products to save time and cost, *SHM* devices used in a structure are commonly customized to cater to the demand and functionality of that particular structure. In addition, the unique requirements of the exterior of structural elements such as fire proofing or indoor appearance requirements hinder the installation of a *SHM* system.

The first *SHM* systems consisted of simple instrumentation. With development in sensor and signal processor technology, *SHM* systems based on these techniques were capable of detecting the structural health of aircrafts and greatly extended the lifetime of aircrafts with the help of a preventive maintenance system (Hickman *et al*. 1991). In 1998, a coordination was achieved between universities, government agencies, and industry, and an innovative *SHM* assessment method for the overall structural condition of structures was proposed by incorporating the basic concept of system identification (Aktan *et al*. 1998).

To reduce both the high cost and time required for the on-site cable installation of a traditional *SHM* system, wireless technology was introduced in the field of *SHM*. For example, a new method combining the advantages of an advanced sensor and the wireless technique was proposed by Pines *et al*., to remotely monitor the condition of various infrastructures in 1998. Data collected by the sensors from a structure can be remotely and wirelessly transmitted back to the server and processed by the *SHM* system on a computer giving an indication of both the damage location and the level of damage (Pines *et al*. 1998). Other *SHM* systems integrating sensors, micro processors, and a wireless transmitter have also been developed, and targets like high speed, accuracy, and low-cost are gradually being accomplished (Tanner 2003, Wang *et al*. 2007).

In subsequent years, a tiny laser scanner installed in different locations of the structure for scanning cracks and monitoring fatigue has been developed. Based on its specific characteristics, the device can be incorporated in aircrafts, railways, and civil structures (Buckner *et al*. 2008). Due to extensive research and subsequent achievements over the past decade, the original *SHM* concept for structures is being used extensively today to monitor specific structure characteristics under both ambient and forced vibrations. A study conducted by Zimmerman *et al*. has also proved that data can be collected reliably and processed by a pure wireless *SHM* system (Zimmerman *et al*. 2008). A *SHM* system based on a hybrid wireless network has also been verified for its feasibility in the laboratory, and several structural response parameters have been effectively monitored on site for a rapid assessment of the conditions (Mascarenas *et al*. 2010).

In addition to the development of the *SHM* system, algorithms focusing on certain specific applications have also been proposed. Contrary to the original concept wherein sensors were installed on the structure to identify the location of the damage, researchers have started to employ customized *SHM* software to enable a more accurate diagnosis. *SHM* software development was initiated in the field of aerospace engineering in the year 2000 to reduce the heavy operating and maintenance fees and to further extend the aircraft lifetime (Boller 2000). Around the same time, various *SHM* algorithms for infrastructures were developed in the field of civil engineering to offer more precise detection results using certain physical *SHM* techniques. For example, Johnson *et al*. utilized local vibration signals in combination with an intelligent diagnosis algorithm to demonstrate the feasibility of a distributed *SHM* system for damage location and monitoring (Johnson *et al*. 2004). Another algorithm based on wavelet analysis to detect the location and the level of damage for the four-story benchmark structure proposed by the American Society of Civil Engineers (*ASCE*) was also developed. The efficacy of this *SHM* system was demonstrated by drawing a comparison with an established finite element model for wind loading (Hera and Hou 2004).

Studies on the selection of proper structural parameters for the *SHM* have been widely conducted over the past decade. Unlike the traditional identification method, parameters selected by the genetic algorithm (*GA*) have shown certain unique advantages of the *SHM* (Udwadia and Proskurowski 1998). The monitoring of large-scale structures is a constant challenge faced by engineers especially when the measured data contains high-frequency noise. Thus, to overcome the above problems, a new statistical *SHM* system based on the Support Vector Machine (*SVM*) was proposed. This system was found to be highly reliable under different types and different levels of noise intensity (Zhang *et al*. 2006). Furthermore, a new method integrating the Autoregressive Moving Average (*ARMA*) models and statistical theory was used to analyze the structural response in the time domain (Carden and Brownjohn 2008). However, as mentioned above, researchers are still faced with the problem of selecting the proper parameters for the *SHM* algorithm.

As the bio-inspired concept was introduced in the field of engineering, researchers began to seek for possible solution inspired from the nature. The concept of gene expression monitoring was first proposed and implemented by Golub (Golub *et al.* 1999). This method offered a new way to classify cancer cells and gave rise to further research in detecting diseases from a gene expression array. The results from the research ignited a new research field, and subsequent research by Slonim *et al*. also demonstrated the feasibility of combining the *NB* algorithm and the *DNA* array data for multi-class cancer diagnosis (Slonim *et al*. 2000). In order to obtain high accuracy and overcome obstacles such as high manpower and high equipment costs for monitoring structures, a new two-mode *SHM* system based on bioinformatics has been proposed in this paper. The proposed system is composed of two main parts: the *SHM* software and *SHM* hardware. The basic theory of the *SHM* algorithm is described in section 2. The preliminary verification of the proposed system is then carried out on an eight-storey downscaled benchmark at *NCREE* in section 3. The proposed *SHM* system is implemented on a mobile *SHM* prototype in section 4. Section 5 discusses the practical verification of the integrated *SHM* system, and based on the results, a summary and conclusion are included.

2. The proposed *SHM* algorithm

As the bio-inspired concept for engineering is a broadly discussed topic, a novel *SHM* algorithm employing array expression data as the Deoxyribonucleic acid (*DNA*) of the structures is proposed in this research. Based on the type of vibration, which can either be strong ground excitation or ambient vibration, the recorded time history is converted using an auto-regression-auto-regression with exogenous (*AR-ARX*) process for micro-vibration and an *ARX* process for earthquake excitation. The *AR* regression model has been proven to be effective in the illustration of the structure model under

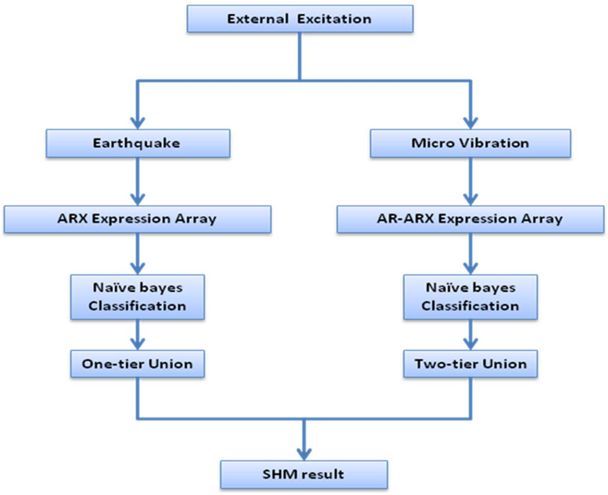

Fig. 1 Flowchart of the *SHM* Algorithm

pure ambient vibration while the *ARX* model is suitable for significant external excitation conditions (Ljung 1986). A series of research conducted by Sohn *et al*. has also demonstrated the advantage of using the chosen *AR-ARX* model for unknown excitation between pure ambient and strong ground excitation (Sohn *et al*. 2000) (Sohn and Farrar, 2001). The obtained array is then compared using the Naïve Bayes (*NB*) classification method, which is the core of the *SHM* algorithm, to detect the damage condition and location as shown in Fig. 1. The basic description of each part is briefly summarized as follows:

2.1 The ARX expression array

The array expression data for earthquake excitation is first extracted using the established *ARX* model. The measured acceleration response is used in the regression model to precisely describe the behavior of the structure.

For a single-input-single-output (*SISO*) system, the relationship between the input and output can be expressed as a linear differential equation given by

$$y(t) + a_1 y(t-1) + \cdots + a_{n_a} y(t-n_a) = b_1 u(t-1) + \cdots + b_{n_b} u(t-n_b) + e(t) \tag{1}$$

Where n_a and n_b represent the output and input steps used for regression, respectively.

As $e(t)$ is commonly treated as a random white-noise error in the differential equation, the model is termed the equation error model, and the adjustable parameters can be shown as

$$\theta = [a_1 \;\; a_2 \cdots a_{n_a} \;\; b_1 \cdots b_{n_b}]^T \tag{2}$$

By assuming

$$A(q) = 1 + a_1 q^{-1} + \cdots + a_{n_a} q^{-n_a} \tag{3}$$

$$B(q) = b_1 q^{-1} + \cdots b_{n_b} q^{-n_b} \tag{4}$$

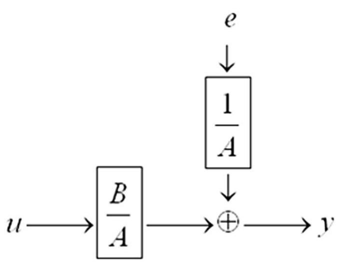

Fig. 2 The *ARX* Model

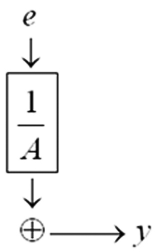

Fig. 3 The *AR* Model

The equation can be rewritten as

$$A(q)\, y(t) = B(q)u(t) + e(t) \tag{5}$$

The regression model described Eq. (5) is a typical example of the *ARX* model shown in Fig. 2 where the *AR* part is denoted by $A(q)\ y\ (t)$, and X is the external input expressed as $B(q)\ u\ (t)$. The model becomes a typical *AR* model if the external excitation X is excluded as depicted in Fig. 3 and will be used as a part of the *AR-ARX* model later on.

2.2 The AR-ARX expression array

The array expression data for the micro-vibration mode of the two-mode *SHM* system is extracted using the two-tier *AR-ARX* model. As the velocity response of the structure is more sensitive compared to the acceleration under conditions of micro-vibration, it is employed in the regression model. The *AR-ARX* model is explained briefly below.

The velocity response $x(t)$ is first input to an *AR* regression model with p terms

$$x(t) = \sum_{j=1}^{p} \phi_{xj} x(t-j) + e_x(t) \tag{6}$$

Where $e_x(t)$ is the white-noise input signal defined as the external excitation of the *AR* model.

By assuming that the error generated from the model depicted in Fig. 2 is the input of Eq. (7), the model combining these two parts represents the proposed *AR-ARX* model illustrated in Fig. 4. The corresponding equation can be expressed as

$$x(t) = \sum_{i=1}^{n_a} a_i x(t-i) + \sum_{j=1}^{n_b} b_j e_x(t-j) + \varepsilon_x(t) \tag{7}$$

Where $e_x(t)$ is the error generated by the first *AR* model; n_a and n_b are the order for the input and output,

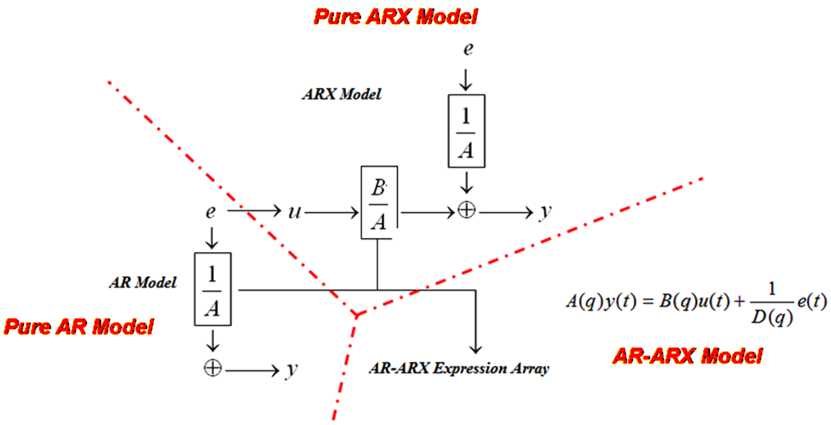

Fig. 4 The *AR-ARX* Model

respectively. The coefficients calculated from the *AR-ARX* model are then used in the micro-vibration mode of the *SHM* system.

2.3 The NAÏVE BAYES (NB) algorithm

The *NB* algorithm, which forms the core of the *SHM* software, is a classification method established on the basics of probability theory. The *a posteriori* probability is estimated from the prior probability and can be expressed as a conditional probability. The test sample is input to the *NB* algorithm with a Bayes probability distribution defined by two parameters, namely, the mean value and standard deviation, to determine the final probability.

The proposed methodology attempts to investigate every coefficient as the *DNA* of the monitoring structure as opposed to the traditional *SHM* method where the health condition is usually determined by only comparing the prediction error of each pre-established regression model. The probability of a specific coefficient of the array expression data is calculated based on the presumed Gaussian distribution for an individual coefficient, which was proven to be easily satisfied. The final damage type is then determined by combining the total probability of the array expression data with the maximum *a posteriori* probability.

The *NB* algorithm can be simplified as

$$Class(x) = arg\ \underset{i}{max}\left\{ \sum_{coefficent} \left[\log(\sigma_i^g) + 0.5\left(\frac{x^g - \mu_i^g}{\sigma_i^g}\right)^2 \right] \right\} \tag{8}$$

Where i is the array number of the test sample; μ_i^g is the mean value of class i and gth coefficient; σ_i^g is the standard deviation of class i and gth coefficient, and x^g is the g^{th} coefficient value of the test sample.

3. Preliminary verification

To verify the feasibility of the proposed *SHM* system in a practical structure, a series of experiments were conducted on the eight-storey downscale specimen at the National Center for Research on

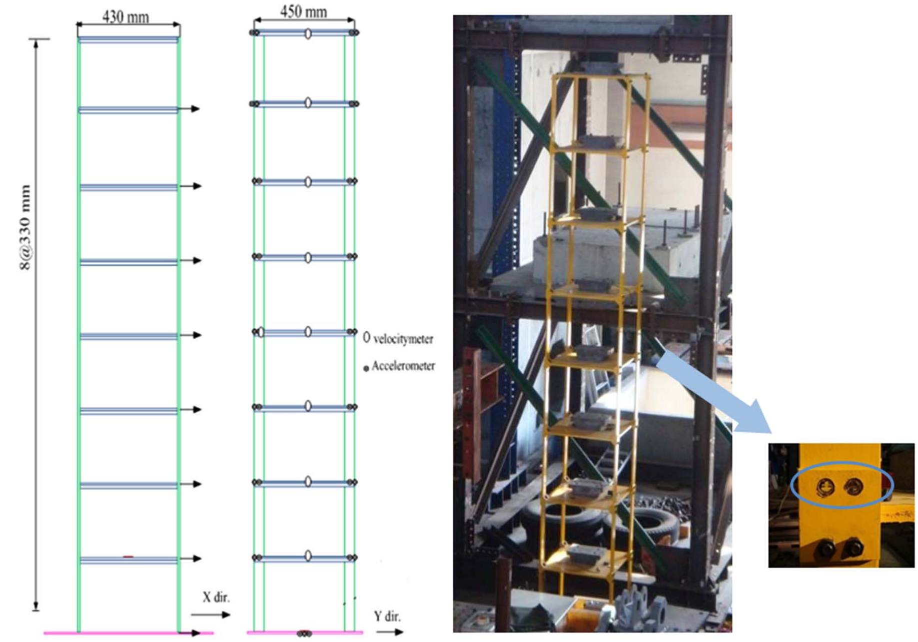

Fig. 5 The eight-story *SHM* Benchmark at *NCREE*

Earthquake Engineering (*NCREE*). As shown in Fig. 5, eight high-sensitivity velocity meters and eight accelerometers were deployed on the specimen to measure the floor response under micro and earthquake vibration conditions with the sampling rate set at 200 Hz.

Signals measured from the ambient vibration in the daily life are first used by the proposed system to enhance its practicability. The structural damages were classified into five major groups for 19 different damage conditions and were simulated by loosening four of the 16 bolts in each floor (1/4 of the beam-column connections). The dataset for the experiment was collected at night to avoid or substantially suppress the unwanted noise arising from machine operation or human activity in the laboratory, which aimed to improve the reliability of the structural feature arrays. The 19 damage conditions are listed in Table 1, and 90 time histories, each subjected to every damage condition for 20 seconds, were recorded. The 19 damage conditions were achieved by switching the location of the loosened fasteners.

Concurrently, the structural response of the benchmark under earthquake excitation conditions was recorded by conducting the shaking table test at *NCREE* to verify the operation of the earthquake mode of the system. A list of the 11 damage conditions achieved by switching the location of the loosened fasteners is listed in Table 2, and 30 time histories including the 1940 El Centro, 1995 Kobe, *TCU* 072 and *TCU* 129 station record of the Chi-Chi earthquake were recorded for different peak ground acceleration (*PGA*) values for every damage condition.

The micro-vibration mode of the *SHM* algorithm was first verified. Three fundamental parameters (p, a, and b) of the basic *AR-ARX* model described in Eqs. (6) and (7) were designed to be 10-8-4 based on the rule of thumb for system identification proposed by Ljung (Ljung 1986). The ratio of the coefficients a and b is set to 2, and the optimal value of p is then determined. Ljung suggests that better identification results can be obtained when the sum of a and b is smaller than p. However, better structural behavior can be achieved by adjusting the value of p from 12 to 10 using an optimization

Table 1 Damage condition for the micro-vibration experiment

Damage condition number	Damage level	Damage location
1	Undamaged	None
2	Slight	1F
3		2F
4		3F
5		4F
6		5F
7		6F
8		7F
9		8F
10	Moderate	1 & 2F
11		3 & 4F
12		5 & 6F
13		7 & 8F
14	Severe	1 & 2 & 3F
15		4 & 5 & 6F
16		6 & 7 & 8F
17	Extreme	1 & 2 & 3 & 4F
18		5 & 6 & 7 & 8F
19	Ultimate	1-8F

Table 2 Damage condition for the earthquake excitation experiment

Damage condition number	Damage level	Damage location
1	Undamaged	None
2	Slight	1F
3		2F
4		3F
5		5F
6		7F
7	Moderate	1 & 2F
8		5 & 6F
9	Severe	1 & 2 & 3F
10		4 & 5 & 6F
11	Ultimate	1 & 2 & 3 & 4F

process.

The advantage of utilizing array expression data for *SHM* was also evaluated using three different array orders, namely, 30-24-12, 40-32-16 and 50-40-20, based on the format specified above to decipher the optimal array for the system while no significant difference of computation overhead was observed. To enable independent testing of the *SHM* system, 10 patterns selected from the database were used to verify the system performance. Fig. 6 depicts the results of all 19 damage conditions, which were obtained from the velocity meter located on the sixth floor (V6). The *AR*-

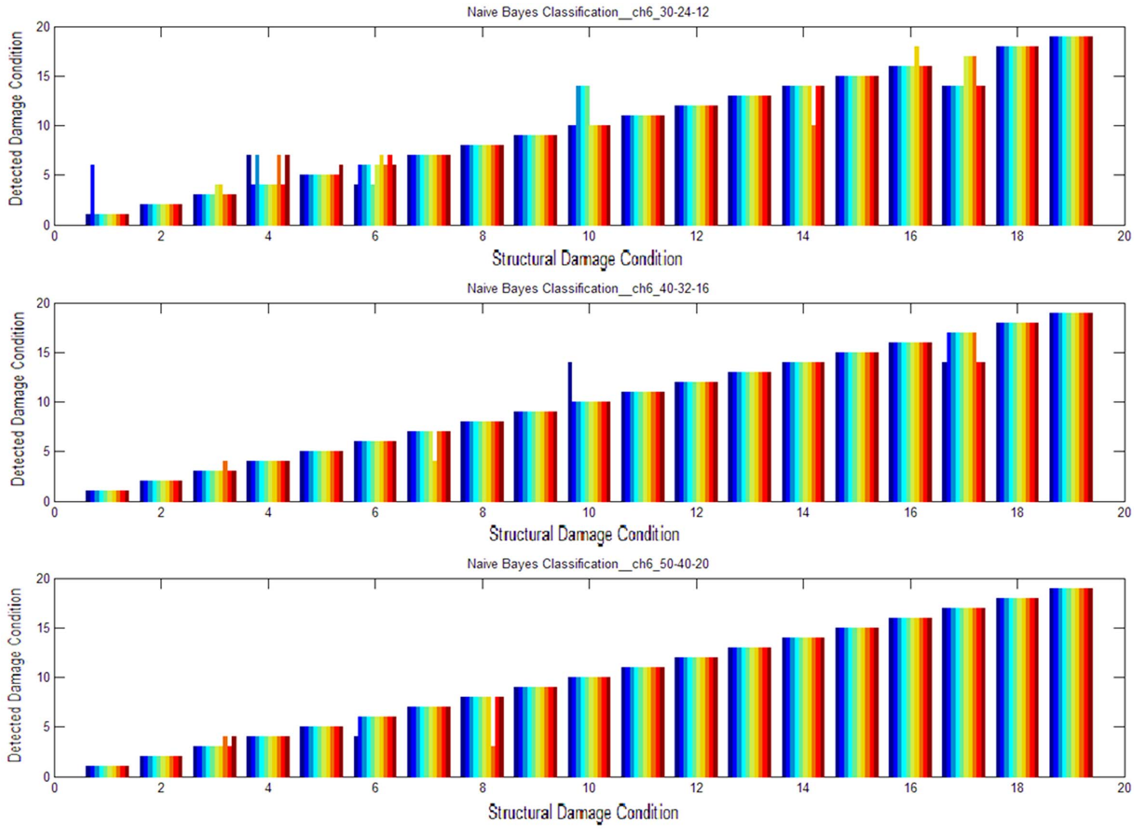

Fig. 6 Verification under micro vibration

ARX order increased from 30-24-12 in the top subplot to the final 50-40-20 in the bottom subplot. The 19 damage conditions are indicated in the longitudinal axis as UN, S1, S2, S3, S4, S5, S6, S7, S8, M12, M34, M56, M78, S123, S456, S678, E1234, E5678, and U12345678 where *UN* represents undamaged; *S* represents slight damage; *M* represents moderate damage; *S* indicates severe damage; *E* indicates extreme damage and *U* indicates ultimate damage. The detected damage condition is reflected in the latitudinal bar. The individual bars for each damage condition express all ten testing patterns. The numbers in the longitudinal axis represents the 19 damage conditions, and the diagnosis result is indicated in the latitudinal axis which should correspond to the same value in the *X*-axis. As demonstrated in Fig. 6, the classification success rate can reach 100% by the proposed system for the 50-40-20 form which can be chosen as the optimal array for micro-vibration except damage conditions 3, 6, and 8 where the success rates are 80%, 90%, and 80%, respectively.

The optimal *ARX* configuration for earthquake excitation conditions was determined using the collected database. Similarly, the two fundamental parameters (*a* and *b*) of the basic *ARX* model described earlier were designed to have a form 8-4. The advantage of utilizing array expression data for *SHM* was again evaluated using three different array orders, namely, 48-24, 56-28, and 64-32 based on the 8-4 form. Five patterns recorded from the established database were used to verify the system performance. The *ARX* order was increased from 48-24 in the top subplot to the final 64-32 form in the bottom subplot. The individual bars as show in Fig. 7 expressed all five testing patterns. The 11 damage conditions are included in the longitudinal axis as *UN*, S1, S2, S3, S5, S7, M12,

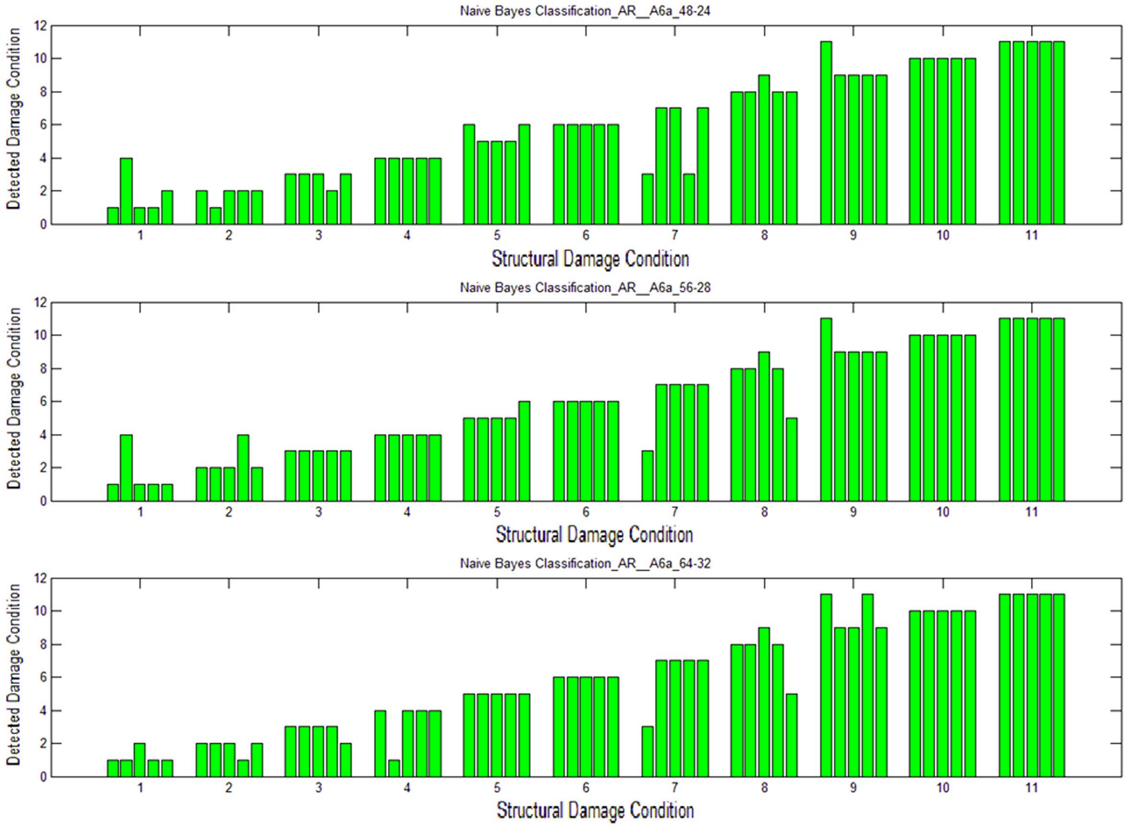

Fig. 7 Verification under earthquake excitation

M56, S123, S456, and U1234 where *UN* represents undamaged; *S* represents slight damage; *M* indicates moderate damage; *S* indicates severe damage, and *U* indicates ultimate damage. Similarly, the latitudinal bar reflects the detected damage condition while the actual damage condition is marked along the longitudinal axis. Structural damage was again correctly predicted by the system for the 64-32 form. The success rates are approximately 60% for damage conditions 8 and 9 and 80% for damage conditions 1, 2, 3, 4, and 7. This array was then chosen to represent the optimal array for earthquake excitation.

The union concept of multi-events or sensors has been introduced to achieve further improvement in the accuracy and reliability of the *SHM* system. The final *SHM* result can be determined by choosing the condition with the highest accumulated probability. Since earthquake excitations are infrequent in occurrence, only the union concept with three sensors was applied for earthquake excitation. Simultaneously, the micro-vibration mode was tested using three sensors on their respective floors (6F, 7F, and 8F) in the first union, and the results of these three different events were then combined to obtain a more accurate result. The verification of the two-mode system is summarized as follows: Table 3 shows the results obtained for earthquake excitation, and Table 4 depicts the outcome of the micro-vibration tests.

As shown in Table 3, the diagnosis result for three separate classes of earthquakes indicates almost the same damage condition and only a slight variation was observed for damage conditions

Table 3 *SHM* result with the union concept under earthquake excitation mode

Damage condition number	Event 1	Event 2	Event 3
1	1	1	2
2	2	2	2
3	3	2	3
4	4	4	4
5	5	5	5
6	6	6	6
7	7	7	7
8	8	8	9
9	11	9	9
10	10	10	10
11	11	11	11

Table 4 *SHM* result with the union concept under micro-vibration mode

Damage condition number	Event 1	Event 2	Event 3	Final result
1	1(1/1/1)	1(1/1/1)	1(1/1/1)	1
2	2(2/2/2)	2(2/2/2)	2(2/2/2)	2
3	3(3/3/3)	3(3/3/3)	3(3/3/4)	3
4	4(4/4/4)	4(4/4/4)	4(4/4/4)	4
5	5(5/5/5)	5(5/5/5)	5(5/5/5)	5
6	6(4/6/6)	6(6/4/6)	6(6/6/6)	6
7	7(7/7/7)	7(7/7/7)	7(7/7/7)	7
8	8(8/8/8)	8(8/8/3)	8(8/8/8)	8
9	9(9/9/9)	9(9/9/9)	9(9/9/9)	9
10	10(10/10/10)	10(10/10/10)	10(10/10/10)	10
11	11(11/11/11)	11(11/11/11)	11(11/11/11)	11
12	12(12/12/12)	12(12/12/12)	12(12/12/12)	12
13	13(13/13/13)	13(13/13/13)	13(13/13/13)	13
14	14(14/14/14)	14(14/14/14)	14(14/14/14)	14
15	15(15/15/15)	15(15/15/15)	15(15/15/15)	15
16	16(16/16/16)	16(16/16/16)	16(16/16/16)	16
17	17(17/17/17)	17(17/17/17)	17(17/17/17)	17
18	18(18/18/18)	18(18/18/18)	18(18/18/18)	18
19	19(19/19/19)	19(19/19/19)	19(19/19/19)	19

1, 3, 8, and 9. However, the approximate damage condition and location can still be rapidly and correctly determined after the occurrence of an earthquake. In addition, a more precise result can be achieved especially in the micro-vibration detection mode. Only a slight error was observed following the application of the first union of the three sensors, and the second-layer union guaranteed a reliable result. In short, the reliability of the two-mode *SHM* system has been demonstrated by the preliminary verification tests indicating that the health condition of the structure under both earthquake excitation and micro-vibration conditions can be accurately detected by the proposed system.

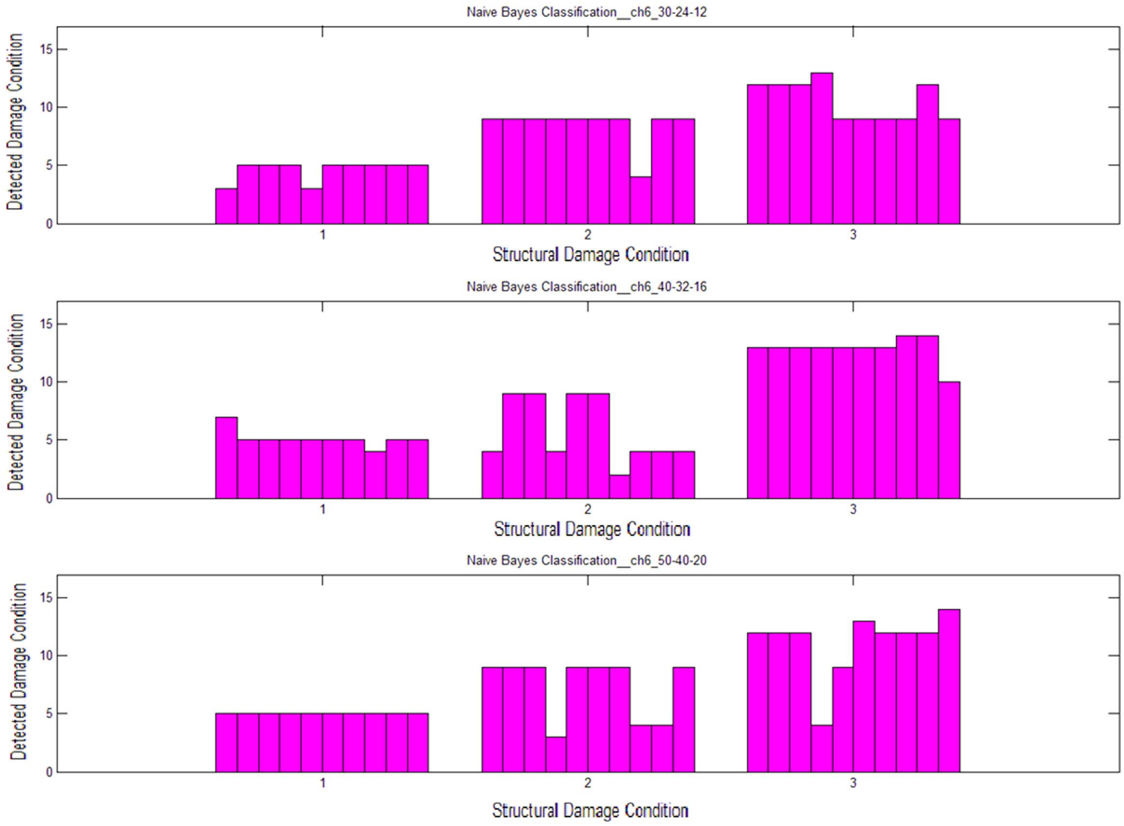

Fig. 8 Verification of unknown damage condition under micro vibration

As mentioned above, the performance of the proposed *SHM* system has been successfully demonstrated in dealing with damage conditions included in the system repository. However, it is impossible to include all possible damage conditions and structure locations into the *SHM* database. To verify the robustness of the proposed *SHM* algorithm, the system was examined by utilizing several damage conditions excluded from the original database. It is expected that the approximate damage condition and location can be detected.

Three damage conditions from both the micro-vibration and earthquake excitation modes were considered, and the rest damage conditions in Tables 1 and 2 were renumbered. For the micro-vibration mode, conditions selected included slight damage on the 5^{th} floor, moderate damage on the 3^{rd} and 4^{th} floors, and severe damage on the 4^{th}& 5^{th}& 6^{th} floors. For the earthquake excitation mode, slight damage on the 7^{th} floor, moderate damage on the 5^{th} and 6^{th} floors, and severe damage on the 4^{th}, 5^{th}, and 6^{th} floors were chosen as the test conditions. The array expression data was input to the *SHM* algorithm to determine the corresponding damage condition. As shown in Fig. 8, the detected damage conditions are indicated by conditions 5, 9 and 12 which reflect the damage condition closest to the actual damage condition with an accuracy of 100%, 70%, and 60%, respectively. Meanwhile, the damage conditions for the earthquake excitation mode shown in Fig. 9 were found to be condition 5, 6, and 7 with an accuracy of 80%, 70%, and 70%, respectively. These results strongly support the reliability of the proposed *SHM* algorithm for use in practical applications wherein the most likely damage condition can be approximated by utilizing the inherent interpolation or extrapolation capability.

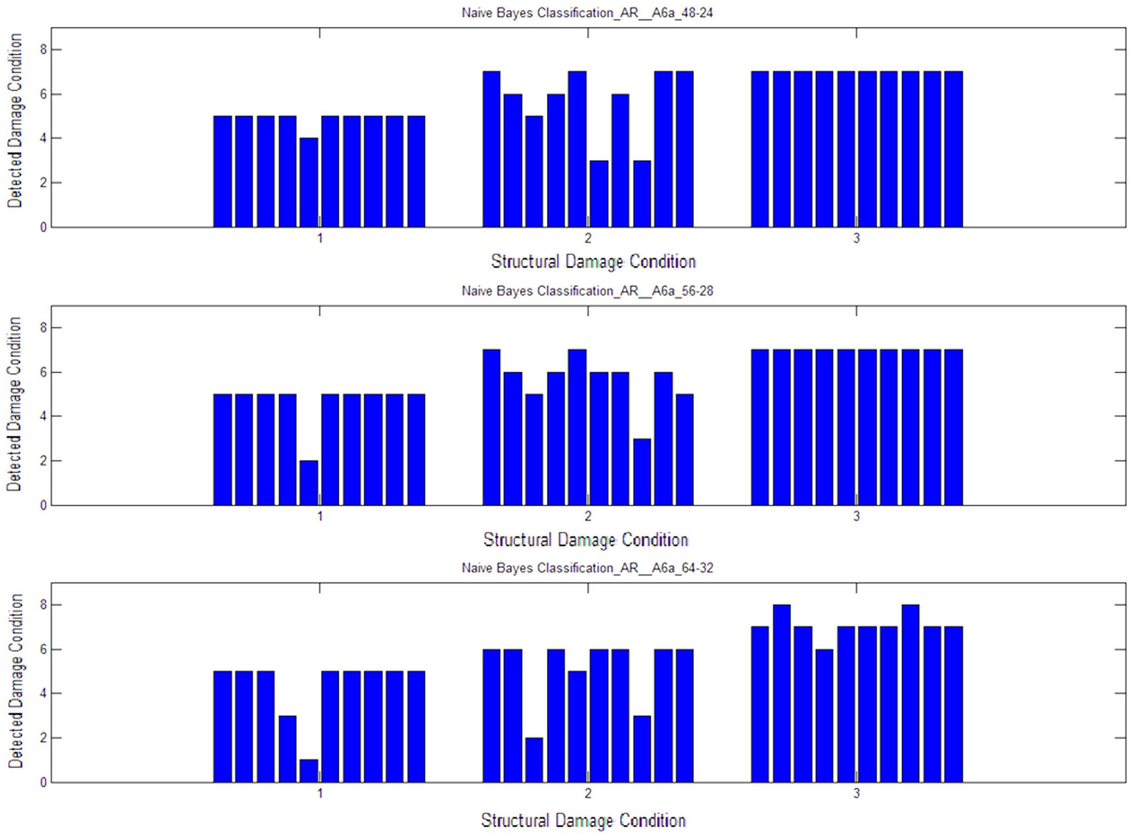

Fig. 9 Verification of unknown damage condition under earthquake excitation

4. Mobile *SHM* prototype

In order to implement the bio-inspired *SHM* system practically, a mobile *SHM* prototype was developed. As shown in Fig. 10, the *SHM* prototype is composed of three fundamental parts including the sensing input module, the *SHM* platform for instrumentation and data processing, and the general packet radio service (*GPRS*) transmission module for conveying the final results to the remote server. To further enhance the mobility of the *SHM* prototype, a customized silver module depicted in Fig. 10 is used for voltage stabilization and power regulation of the sensing unit and data processing center. The vibration data is first measured by the deployed sensor and is subsequently transmitted through the input module to the built-in microprocessor. The acceleration and velocity of the structure are both measured simultaneously to evaluate its structural health condition. In addition, by connecting multiple *SHM* prototypes, the system can be extended to form a *SHM* network.

The details of the customized sliver module are shown in Fig. 11. A total of seven connectors are mounted in the box. Both the velocity meter and the accelerometer can be connected to the two sensor connectors located in the rightmost column for different applications. For the micro-vibration mode, two measurement resolutions can be selected by using the built-in 10 V/Kine or 1 V/Kine

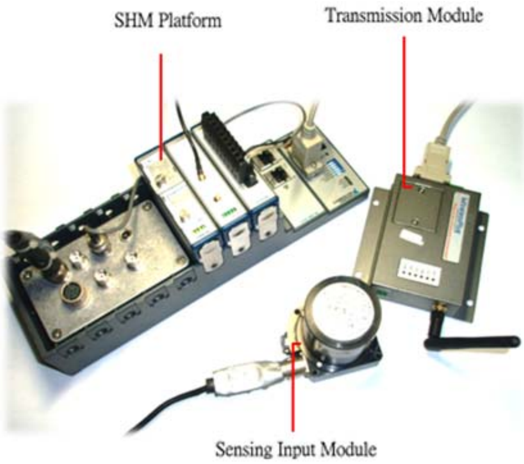

Fig. 10 The *SHM* Prototype

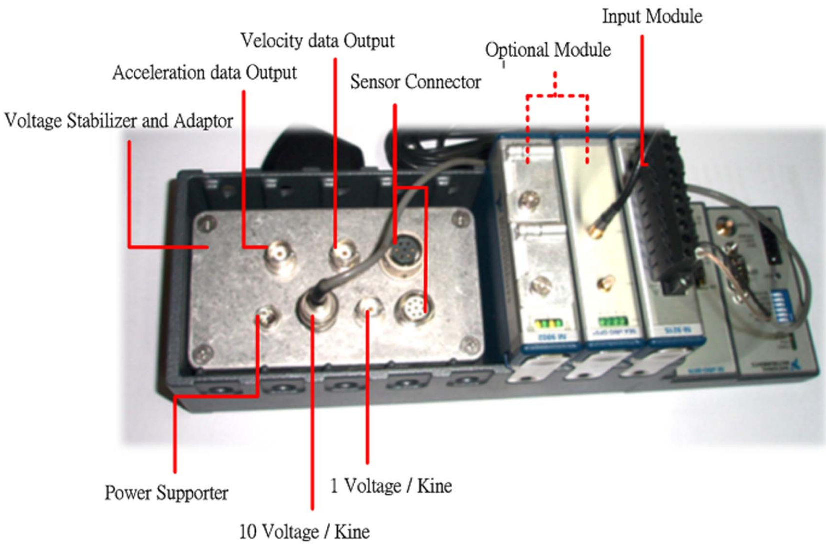

Fig. 11 The *SHM* Monitoring Platform

converters. Up to 16 sensors can be powered simultaneously by the customized unit. In addition, two optional modules, a *GPS* module and a memory card module for depositing the collected raw data, can be installed adjacent to the input module. These two modules enable an easy extension of the functionality and mobility of the platform.

In order to correctly execute the proposed algorithm in the prototype, the *SHM* algorithm is incorporated in the firmware of the mobile module. The corresponding software can be divided into two parts: the onsite program in the *SHM* platform and the demonstration program in the remote server where all the structure damage information is collected and displayed. As shown in Fig. 12, the on-site program is further subdivided into four parts: Data Pre-Processing, Coefficient Extraction, Health Condition Diagnosis, and *GPRS* & Wireless Module.

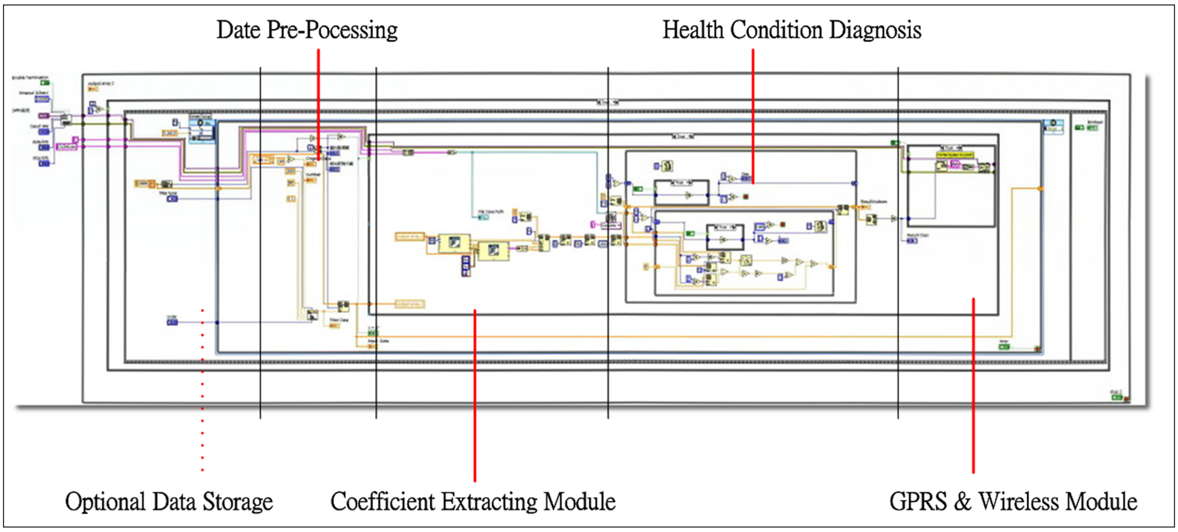

Fig. 12 The on-site program

4.1 Data pre-processing

The Pre-Processing program performs three main functions: input data collection, digital filter design, and data size adjustment/setting for *SHM* processing. The use of the Pre-Processing program helps to eliminate the undesired noise successfully from the ambient environment to ensure clarity in the input data. In this study, the data sample rate was selected as 200 Hz, and a band-pass filter was chosen to filter out the unwanted high and low frequency sets of 90 Hz and 0.1 Hz. This also helped to eliminate errors arising from the voltage conversion between the analog and digital signals to enable accurate collection of desired data.

4.2 Coefficient extraction module

The Coefficient Extraction module was designed based on the two proposed *SHM* algorithms. In this study, the *ARX* and *AR-ARX* models are first established and then implemented with the desired order of settings. The Coefficient Extraction module assists in transforming the time history of the structural responses into array form quickly, and the damage condition of the structure can subsequently be evaluated in the next stage by making a comparison between the damage data and the collected database.

4.3 Health condition diagnosis

The condition and location of the structural damage are determined by the embedded *NB*-based *SHM* algorithm. By making a comparison between the arrays calculated from the previous block and the stored database, the probability of occurrence of all damage conditions for either earthquake excitation or micro-vibration modes is estimated by a designated loop which subsequently enables the detection of the location and condition of the structural damage.

4.4 GPRS & wireless module

In order to achieve the goal of real-time monitoring following the analysis and classification of the damage, the *GPRS* Module is used to transfer the data back to the monitoring server. To ensure the security of the data being transmitted, a technique to safely encrypt and decrypt the data by adding an initial *AA* string at the beginning of data transmission chain was developed. Only data with are equipped with this characteristic will then be received.

The mobile *SHM* prototype can be applied to real life structures by combining the software and hardware described above. By utilizing the mobile *SHM* prototype designed, the structural damage condition can be classified within a span of one minute.

5. Practical verification

The performance of the *SHM* prototype was tested using experimental verification. The eight-storey, downscaled benchmark at *NCREE* was used as the practical test structure. Structural damage testing was simulated by loosening four bolts on the third floor which represented damage condition 4. The

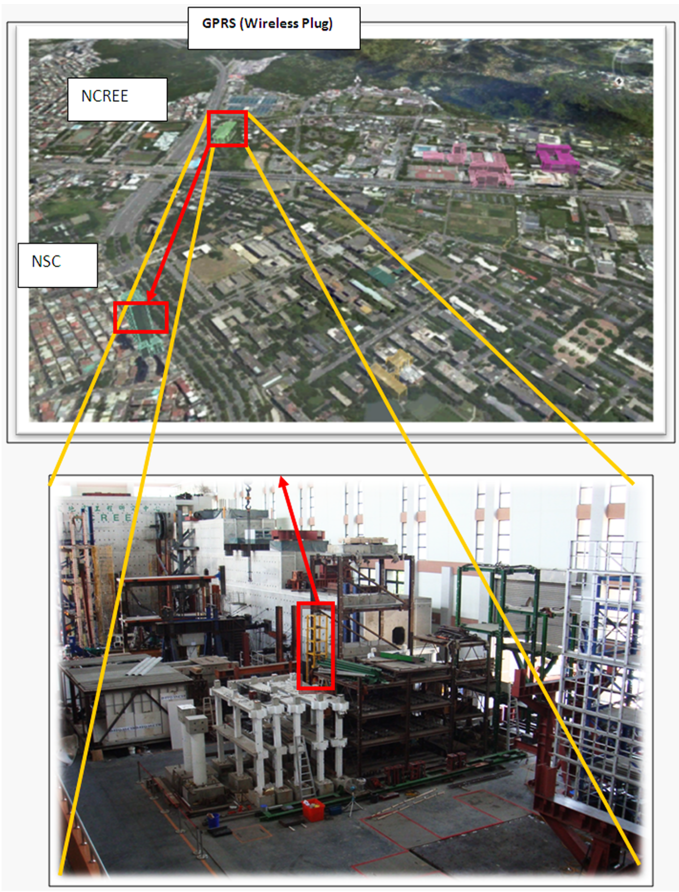

Fig. 13 Location of the benchmark and the monitoring server

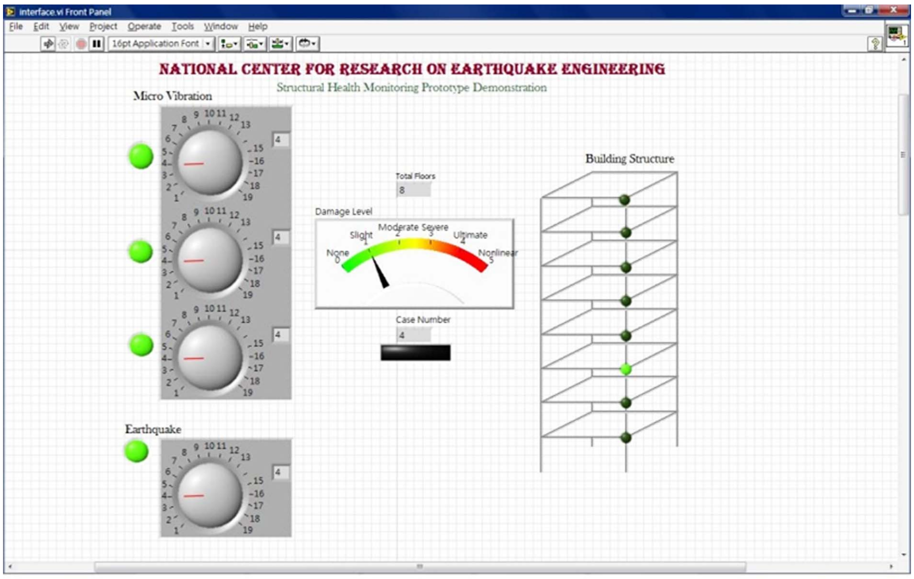

Fig. 14 The real-time monitoring interface

response under both ambient and earthquake vibration modes was measured using the top three sensors (6F, 7F, and 8F) deployed on the structure.

By comparing the *AR-ARX* and *ARX* array obtained from the vibration data with the database deposited in the on-site *SHM* prototype, the structural health condition can be immediately evaluated. In addition, to demonstrate the feasibility of remote monitoring, the server was chosen at the headquarters of the National Science Council (*NSC*), and the health condition of the structure was immediately transmitted by the *GPRS* service since the proposed *SHM* system only requires a small bandwidth. The locations of the benchmark and the monitoring server are shown in Fig. 13.

The result from real-time monitoring is shown in Fig. 14. It shows that *SHM* results can be determined by either the earthquake mode or the micro-vibration mode. The switching criterion between these two modes is set to an acceleration of 5 gal. If the largest measured acceleration is less than 5 gal, the structural response is measured and processed every 20 seconds, and the results are displayed sequentially in the top left-hand portion of the figure. The numbers shown in the panel represent the classification result. As mentioned in the previous section, to avoid false alarms in practical applications, the *SHM* algorithm operates three times a minute with the two-layer union concept to determine the condition and location of the structure damage as depicted in Fig. 14. The damage level of the structure is either none, slight, moderate, severe, extreme, or ultimate, and is shown in the middle of the figure. The detected damage location is highlighted on the structure. In addition, the *SHM* system was also tested by shaking the benchmark structure under earthquakes. The earthquake mode was launched once the detected acceleration value became greater than 5 gal. The union result from the three different sensors is shown in the bottom-left hand corner of Fig. 14. The experiment result clearly demonstrated that both the damage condition, which was slight, and the location, i.e., the third floor, could be detected with precision by the two-mode *SHM* system.

In addition, not only can real-time structural damage be monitored by the mobile *SHM* prototype, the embedded parameters can also be remotely controlled. This flexible monitoring design can make the *SHM* system an optimal system for facilitating varied conditions and permit the immediate evaluation of any structural damage. Characteristics like high mobility and prompt on-site processing of the proposed mobile *SHM* system have finally been implemented.

6. Conclusions

A bio-inspired two-mode *SHM* system based on the *NB* classification method was presented in this paper. Since research focus on the bio-inspired concept for engineering has only recently evolved, a novel *SHM* algorithm utilizing the array expression data of the *DNA* of the structures was developed. Based on the vibration mode, the proposed *SHM* algorithm can switch between a two-tier *AR-ARX* process for micro-vibration and an *ARX* process for earthquake excitation. The health condition of the structure is then determined by classifying the obtained array expression data using the *NB* method. Moreover, the union concept in probability was introduced to improve the accuracy of the system.

To verify the performance and reliability of the *SHM* algorithm, a downscaled eight-storey steel building located at the shaking table of *NCREE* was used as the benchmark structure. The structural damage was simulated by loosening four of the 16 bolts in each floor (1/4 of the beam-column connection). The structural response was then determined for different damage levels and locations for inclusion in the structural health monitoring database. Experimental results have demonstrated that the approximate condition and location of the damage can be quickly determined immediately after the occurrence of an earthquake. A more precise result can be achieved in the micro-vibration detection mode.

To implement the proposed *SHM* system in a practical application, a *SHM* prototype consisting of three individual modules, namely, the input sensing module, the transmission module, and the *SHM* platform was developed. The employed sensor first measures the structural response, and subsequently the *SHM* mode corresponding to the excitation is chosen automatically by the system to rapidly evaluate the health condition of the structure using a preset criterion. Test results from the ambient vibration and shaking table test have shown that the condition and location of the benchmark structure damage can be successfully monitored by the *SHM* prototype system and can be instantly transmitted to a remote server to facilitate real-time monitoring.

Implementing the bio-inspired two-mode *SHM* practically has been demonstrated in this paper. The bio-inspired concept is made possible by the successful integration of software and hardware. With its unique mobility and powerful processing capacity, it is expected that the proposed *SHM* system can be extended to *SHM* networks in practical applications in the near future.

Acknowledgements

This research was sponsored in part by the National Science Council of R.O.C. (Taiwan) through grants 98-2815-C-492-001-E and 98-2815-C-002-033-E. This support is gratefully acknowledged. The authors are also grateful to the *NCREE*, Taiwan for their technical support with regards the shaking table tests.

References

Hickman, G.A., Gerardi, J.J. and Feng, Y. (1991), "Application of smart structures to aircraft health monitoring", *J. Intel. Mat. Syst. Str.*, **2**(3), 411-430.

Aktan, A.E., Helmicki, A.J. and Hunt, V.J. (1998), "Issues in health monitoring for intelligent infrastructure", *Smart Mater. Struct.*, **7**(5), 674-92.

Pines, D.J. and Lovell, P.A. (1998), "Conceptual framework of a remote wireless health monitoring system for large civil structures", *Smart Mater. Struct.*, **7**(5), 627-36.

Tanner, N.A., Wait, J.R., Farrar, C.R. and Hoon, S. (2003), "Structural health monitoring using modular wireless sensors", *J. Intel. Mat. Syst. Struct.*, **14**(1), 43-56.

Wang, Y., Lynch, J.P. and Law, K.H. (2007), "A wireless structural health monitoring system with multithreaded sensing devices: Design and validation", *Struct. Infrastruct. E.*, **3**(2), 103-120.

Lynch, J.P., Law, K.H., Kiremidjian, A.S., Carryer, E., Farrar, C.R., Sohn, H., Allen, D.W., Nadler, B. and Wait, J.R. (2004), "Design and performance validation of a wireless sensing unit for structural monitoring applications", *Struct. Eng. Mech.*, **17**(3-4), 393-408.

Buckner, B.D., Markov, V., Li-Chung, L. and Earthman, J.C. (2008), "Laser-scanning structural health monitoring with wireless sensor motes", *Opt. Eng.*, **47**(5), 1-9.

Zimmerman, A.T., Shiraishi, M., Swartz, R.A. and Lynch, J.P. (2008), "Automated modal parameter estimation by parallel processing within wireless monitoring systems", *J. Infrastruct. Syst.*, **14**(1), 102-113.

Mascarenas, D.D.L., Flynn, E.B., Todd, M.D., Overly, T.G., Farinholt, K.M., Park, G. and Farrar, C.R. (2010), "Development of capacitance-based and impedance-based wireless sensors and sensor nodes for structural health monitoring applications", *J. Sound Vib.*, **329**(12), 2410-2420.

Boller, C. (2000), "Next generation structural health monitoring and its integration into aircraft design", *Int. J. Syst. Sci.*, **31**(11), 1333-49.

Hu, N., Wang, X., Fukunaga, H., Yao, Z.H., Zhang, H.X. and Wu, Z.S. (2001), "Damage assessment of structures using modal test data", *Int. J. Solids Struct.*, **38**(18), 3111-3126.

Johnson, T.J., Brown, R.L., Adams, D.E. and Schiefer, M. (2004), "Distributed structural health monitoring with a smart sensor array", *Mech. Syst. Signal Pr.*, **18**(3), 555-72.

Hera, A. and Hou, Z. (2004), "Application of wavelet approach for ASCE structural health monitoring benchmark studies", *J. Eng. Mech.*, **130**(1), 96-104.

Udwadia, F.E. and Proskurowski, W. (1998), "A memory-matrix-based identification methodology for structural and mechanical systems", *Earthq. Eng. Struct. D.*, **27**(12), 1465-1481.

Zhang, J., Sato, T. and Iai, S. (2006), "Support vector regression for on-line health monitoring of large-scale structures", *Struct. Safety*, **28**(4), 392-406.

Carden, E.P. and Brownjohn, J.M.W. (2008), "ARMA modelled time-series classification for structural health monitoring of civil infrastructure", *Mech. Syst. Signal Pr.*, **22**(2), 295-314.

Sohn, H., Czarnecki, J.A. and Farrar, C.R. (2000), "Structural health monitoring using statistical process control", *J. Struct. Eng.*, **126**(11), 1356-1363.

Sohn, H. and Farrar, C.R. (2001), "Damage diagnosis using time series analysis of vibration signals", *Smart Mater. Struct.*, **10**(3), 446-51.

Ljung, L. (1986), "System identification: theory for the user", Prent-Hall, Inc. Upper Saddle River, NJ, USA.

Golub, T.R., Slonim, D.K., Tamayo, P., Huard, C., Gaasenbeek, M., Mesirov, J.P., Coller, H., Loh, M.L., Downing, J.R., Caligiuri, M.A., Bloomfield, C.D. and Lander, E.S. (1999), "Molecular classification of cancer: class discovery and class prediction by gene expression monitoring", *Science*, **286**(5439), 531-537.

Donna, K.S., Pablo, T., Jill, P.M., Todd, R.G. and Eric, S.L. (2000), "Class prediction and discovery using gene expression data", Annual Conference on Research in Computational Molecular Biology, *Proceedings of the 4th annual international conference on Computational molecular biology*, 263-272, 1-58113-186-0, Tokyo.